Scattering of Electrons by C, N, O, N^+, O^+, and O^{++}†*

Ronald J. W. Henry
Space Division, Kitt Peak National Observatory,‡ Tucson, Arizona 85717
and
P. G. Burke and A.-L. Sinfailam
Department of Applied Mathematics, Queens University, Belfast, North Ireland
(Received 3 September 1968)

The formulation given by Smith *et al.*, for transitions induced by electron impact among ground-state terms of atoms or ions with configurations $2p^q$ or $3p^q$, is corrected. Close-coupling equations are solved numerically for electrons incident on C, N, O, N^+, O^+, and O^{++}. Shape resonances are found in low-energy elastic scattering by ground-state carbon and nitrogen atoms. Peaks in electron-atom inelastic cross sections are found to occur at lower energies than those calculated by Smith *et al.*, and the magnitude of the cross sections is lower at high energies. Collision strengths for electron scattering by O^+, N^+, and O^{++} are presented.

I. INTRODUCTION

A theory for describing transitions induced by electron impact among all the ground-state terms of atoms and ions with configurations np^q, where $n=2$ or 3 and $0 \leq q \leq 6$, was given by Smith, Henry, and Burke.[1] Their analysis was applied to calculations[2] of elastic and inelastic cross sections for electrons incident on atomic carbon, nitrogen, and oxygen. However, these calculations must be modified, since an error was made in the antisymmetrization of certain terms in the total wave function. With the correct formulation, we obtain shape resonances in low-energy elastic scattering by carbon and nitrogen. We also present collision strengths for electron scattering by O^+, N^+, and O^{++}.

In the expansion of the total wave function for these electron-atom and electron-ion systems, only terms belonging to the ground-state configurations are retained. We then solve the close-coupling equations numerically using the method outlined in Ref. 1.

The corrections in the theory are presented in Sec. II. In Sec. III, the corrected cross sections for electron-atom scattering are given, and the resulting low-energy shape resonances are discussed in detail in Sec. IV. The collision strengths for electron-ion scattering are given in Sec. V, followed by the principal conclusions in Sec. VI.

II. THEORY

The total wave function[1] for an electron-atom system, where the atom has one unfilled p shell with configuration $2p^q$ or $3p^q$, can be written as

$$\Psi(\Gamma_j;\vec{x}) = \sum_{k=1}^{N+1} (-1)^{N+1-k}(N+1)^{-\frac{1}{2}} \times \sum_{\Gamma_i} \Phi(1s^2 2s^2 \ldots np^q L_i S_i k_i l_i LS; \vec{x}-k\, \hat{r}_k \sigma_k) F_{ij}(r_k) r_k^{-1} + c_j \Psi_0(1s^2 2s^2 \ldots np^{q+1} LS; \vec{x}). \quad (1)$$

In this equation $\vec{x}$ denotes the space and spin coordinates of all $(N+1)$ electrons: $\vec{x}-k$ denotes the space and spin coordinates of all the electrons except the kth: Φ is constructed from the Hartree-Fock solution for the atom and the angular and spin parts of the wave function of the kth electron: $F_{ij}(r_k)$ is the function describing the radial motion of the incident electron: Ψ_0 is a term which allows for that component of the incident-electron wave function which is in the unfilled p orbital: $\Gamma_j = \gamma_j k_j l_j L_j S_j LSM_L M_S$ denotes the jth channel, where $\gamma_j L_j S_j$ defines the atomic state, $k_j l_j$ defines the incident-electron state, and L and S are the total orbital momentum and total spin of the electron-atom system, respectively. The functions $F_{ij}(r)$ satisfy a system of coupled integro-differential equations with boundary conditions

$$\begin{aligned} &F_{ij}(0) = 0, \\ &F_{ij}(r) \sim k_i^{-1/2}(\delta_{ij} \sin\theta_i + R_{ij} \cos\theta_i), \quad \text{as } r\to\infty, \quad k_i^2 > 0, \\ &\quad \sim N_{ij} \exp(-|k_i|r - |\eta_i| \ln 2k_i r), \quad \text{as } r\to\infty, \quad k_i^2 > 0, \end{aligned} \quad (2)$$

where $\theta_i = k_i r - \frac{1}{2} l_i \pi - \eta_i \ln 2k_i r + \sigma_{l_i}$, $\eta_i = -(Z-N)/k_i$,

$\sigma_{l_i} = \arg\Gamma(l_i + 1 + i\eta_i)$, and $k_i^2 = 2(E - E_i)$.

Here E is the total energy and E_i is the energy of the atom in the state $\gamma_i L_i S_i$. From the asymptotic form of $F_{ij}(r)$, the matrix R_{ij} can be determined and the cross section evaluated in the usual manner.[3]

The function Ψ_0 in Eq. (1) allows considerable simplification of the exchange terms since it is possible to write

$$\langle P_{np} | F_{ij} \rangle = 0, \quad \text{for } l_i = 1, \tag{3}$$

as well as the usual orthogonality to closed shells. The derivation of the equations satisfied by the functions $F_{ij}(r)$, follows from the Kohn variational principle

$$\delta(\underline{I} - \tfrac{1}{2}\underline{R} + 2\underline{D} \cdot \langle P_{np} | \underline{F} \rangle) = 0, \tag{4}$$

where $\underline{D} = d_i \delta_{ij} \delta_{li\,1}$ is a diagonal matrix of Lagrangian multipliers which are required to ensure that Eq. (3) is satisfied. The matrix $\underline{I}$ is defined by

$$I_{ij} = \int \Psi^*(\Gamma_i; \vec{x})(H - E)\Psi(\Gamma_j; \vec{x}) d\vec{x}, \tag{5}$$

and the variation δ in Eq. (4) is taken with respect to the functions F_{ij}, subject to the boundary conditions given by Eq. (2). In Ref. 1, an error was made in the evaluation of the terms involving Ψ_0. The corrected form of the equations satisfied by $F_{ij}(r)$ may be given as

$$\sum_j \mathfrak{L}_{ij} F_{jk}(r) + (E - E_{N+1})^{-1} V_i(r) \sum_j \int V_j(r') F_{jk}(r') dr' + d_i P_{np}(r) \delta_{l_i 1} = 0, \tag{6}$$

where $\mathfrak{L}_{ij} = -\frac{1}{2}\left(\frac{d^2}{dr^2} - \frac{l_i(l_i+1)}{r^2} + \frac{2Z}{r} + k_i^2\right)\delta_{ij} + V_{ij}(r) + W_{ij}(r)$, (7)

$$V_{ij}(r) = \delta_{ij} \sum_{\substack{n'l' = \text{closed} \\ \text{subshells}}} 2(2l'+1) Y_0(P_{n'l'} P_{n'l'}; r) + 3q\delta_{S_i S_j} [(2l_i+1)(2l_j+1)(2L_i+1)(2L_j+1)]^{1/2}$$

$$\times \sum_\lambda (2\lambda+1)^{-1} C(l_i l_j \lambda; 000) C(11\lambda; 000) W(l_i L_i l_j L_j; L\lambda)$$

$$\times \sum_{L_2 S_2} (-1)^{L_2 + L + L_i + L_j} W(1L_i 1L_j; L_2\lambda)(qL_i S_i | \} L_2 S_2)(qL_j S_j | \} L_2 S_2) Y_\lambda(P_{np} P_{np}; r), \tag{8}$$

$$W_{ij}(r) F_{jk}(r) = -\delta_{ij} \sum_{\substack{n'l' = \text{closed} \\ \text{subshells}}} \sum_\lambda (2l'+1)(2l_i+1)^{-1} C(l'\lambda l_i; 000)^2$$

$$\times Y_\lambda(P_{n'l'} F_{jk}; r) P_{n'l'}(r) - 3q[(2l_i+1)(2l_j+1)(2L_i+1)(2L_j+1)(2S_i+1)(2S_j+1)]^{1/2}$$

$$\times \sum_{L_2 S_2} (qL_i S_i | \} L_2 S_2)(qL_j S_j | \} L_2 S_2) W(S_j \tfrac{1}{2} \tfrac{1}{2} S_i; S S_2)$$

$$\times \sum_\lambda (2\lambda+1)^{-1} C(1 l_j \lambda; 000) C(l_i 1\lambda; 000) X(1L_2 L_i; l_j L_j L; \lambda 1 l_i) Y_\lambda(P_{np} F_{jk}; r) P_{np}(r), \tag{9}$$

$$V_i(r) = (q+1)^{1/2} \delta_{l_i 1} (q+1 LS | \} L_i S_i) \Bigg[-\frac{1}{2}\left(\frac{d^2}{dr^2} - \frac{2}{r^2} + \frac{2Z}{r}\right) P_{np}(r)$$

$$+ \sum_{\substack{n'l' = \text{closed} \\ \text{channels}}} [2(2l'+1) Y_0(P_{n'l'} P_{n'l'}; r) P_{np}(r)$$

$$- \tfrac{1}{3} \sum_\lambda (2l'+1) C(l'\lambda 1; 000)^2 Y_\lambda(P_{n'l'} P_{np}; r) P_{n'l'}(r)] \Bigg]$$

$$+3q(q+1)^{1/2}\sum_{L'S'}\delta_{S'S_i}(q+1LS|\}L'S')[3(2l_i+1)(2L'+1)(2L_i+1)]^{1/2}$$
$$\times\sum_{L_2S_2}(-1)^{L_2+L+L'+L_i}(qL'S'|\}L_2S_2)(qL_iS_i|\}L_2S_2)$$

$$\times\sum_\lambda(2\lambda+1)^{-1}C(11\lambda;000)C(1l_i\lambda;000)W(1L'l_iL_i;L\lambda)W(1L'1L_i;L_2\lambda)Y_\lambda(P_{np}P_{np};r)P_{np}(r), \tag{10}$$

and

$$E_{N+1}=\sum_{\substack{n'l'=\text{all}\\ \text{subshells}}}\left(-\frac{1}{2}\right)N_{n'l'}\int P_{n'l'}(r)\left(\frac{d^2}{dr^2}-\frac{l'(l'+1)}{r^2}+\frac{2Z}{r}\right)P_{n'l'}(r)dr$$

$$+\sum_{\substack{n'l'=\text{closed}\\ \text{subshells}}}\tfrac{1}{2}N_{n'l'}(N_{n'l'}-1)[R_0(P_{n'l'}{}^4)-\tfrac{2}{25}\delta_{l'1}R_2(P_{2p}{}^4)]+\sum_{\substack{n''l''>n'l'=\text{all}\\ \text{subshells}}}N_{n''l''}N_{n'l'}$$
$$\times\left(R_0(P_{n''l''}P_{n'l'}P_{n''l''}P_{n'l'})-\tfrac{1}{2}\sum_\lambda(2\lambda+1)^{-1}C(l'l''\lambda;000)^2R_\lambda(P_{n''l''}P_{n'l'}P_{n'l'}P_{n''l''})\right)$$
$$+\tfrac{9}{2}q(q+1)\sum_{L'S'L''}(q+1LS|\}L'S')(q+1LS|\}L''S')[(2L'+1)(2L''+1)]^{1/2}$$
$$\times\sum_{L_2S_2}(-1)^{L_2+L+L'+L''}(qL'S'|\}L_2S_2)(qL''S'|\}L_2S_2)$$
$$\times\sum_\lambda(2\lambda+1)^{-1}C(11\lambda;000)^2W(1L'1L'';L_2\lambda)W(1L'1L'';L\lambda)R_\lambda(P_{np}{}^4). \tag{11}$$

Here N_{nl} is the number of electrons in the nl subshell, and the remaining notation is given in Ref. 1. The X coefficient in Eq. (9) is defined by

$$X(abc;\,pqr;\,xyz)=(-1)^s\sum_t(2t+1)W(bpcx;ta)W(pbry;tq)W(xcyr;tz),$$

where $s=a+b+c+p+q+r+x+y+z$.

The direct and exchange potentials, V_{ij} and W_{ij}, respectively, are unchanged, but the expressions for V_i and E_{N+1} differ from those given in Ref. 1. These differences have also been discussed by Smith, Conneely, and Morgan.[4] We agree with their expressions, except for some differences in $V_i(r)$.

Recently, there has been some discussion concerning the signs of the fractional parentage coefficients $(qLS|\}L'S')$ for the p shell.[5] Table I gives the values which we use in the calculations reported below. These differ from the set used in our earlier calculations, and cause some of the signs of the off-diagonal elements of the R matrices to be changed. However, the cross sections are not modified by the changes in signs.

III. ELECTRON-ATOM RESULTS

Because of the changes in $V_i(r)$ and E_{N+1}, our results for the cross sections for electron scattering by carbon, nitrogen, and oxygen differ from those presented in Ref. 2. Since these changes occur in the treatment of Ψ_0 in Eq. (1), only those LS states which are allowed in the np^{q+1} configuration are affected.

We present our new results, as a function of energy above the inelastic threshold, for forbidden excitations in e^--C, e^--N, and e^--O scattering, in Figs. 1–3, respectively. In these calculations we have used the Hartree-Fock energy for the ground state of the atom, and experimental values for the energy differences between the atomic levels. We compare our results with the earlier calculations, which are denoted by dashed curves in the figures. The main effects of the changes are to cause the peaks in the cross sections to occur at lower energies, and to lower the cross sections at higher energies. At high energies, the spin-forbidden cross sections approach the asymptotic behavior of E^{-3}, and the electric dipole and electric quadrupole cross sections fall off as $E^{-1}\ln E$ and E^{-1}, respectively. The coefficients for this asymptotic energy behavior are given in Table II.

The total cross sections for scattering of electrons by the ground state of atoms are compared with our earlier work (dashed curves) in Fig. 4. The change in our results for atomic oxygen is negligible, and so the theoretical cross section near the threshold still lies about a factor of two higher than the experimental results of Sunshine *et al.*[6] This discrepancy is due to our neglect of

TABLE I. Fractional parentage coefficients $(qL_iS_i|\}L_jS_j)$ for the p shell.

$q=1$	$i\backslash j$	^1S
	^2P	1

$q=2$	$i\backslash j$	^2P
	^3P	1
	^1D	1
	^1S	1

$q=3$	$i\backslash j$	^3P	^1D	^1S
	^4S	1	0	0
	^2D	$-1/\sqrt{2}$	$1/\sqrt{2}$	0
	^2P	$-1/\sqrt{2}$	$-\sqrt{5}/3\sqrt{2}$	$\sqrt{2}/3$

$q=4$	$i\backslash j$	^4S	^2D	^2P
	^3P	$-1/\sqrt{3}$	$-\sqrt{5}/2\sqrt{3}$	$-1/2$
	^1D	0	$\sqrt{3}/2$	$-1/2$
	^1S	0	0	1

$q=5$	$i\backslash j$	^3P	^1D	^1S
	^2P	$\sqrt{3}/\sqrt{5}$	$1/\sqrt{3}$	$1/\sqrt{3}\sqrt{5}$

$q=6$	$i\backslash j$	^2P
	^1S	1

polarization potential terms, which are particularly important in calculations of s-wave elastic scattering cross sections for atomic oxygen. Henry[7] has shown that when these extra terms are included, the cross section at threshold is decreased by more than a factor of 2.

For atomic nitrogen, experimental total cross sections were obtained by Neynaber *et al.*[8] in the energy range 1.6–10.0 eV. In this range, our theoretical values lie above those of experiment. The inclusion of polarization terms may bring the energy dependence of the two curves into good

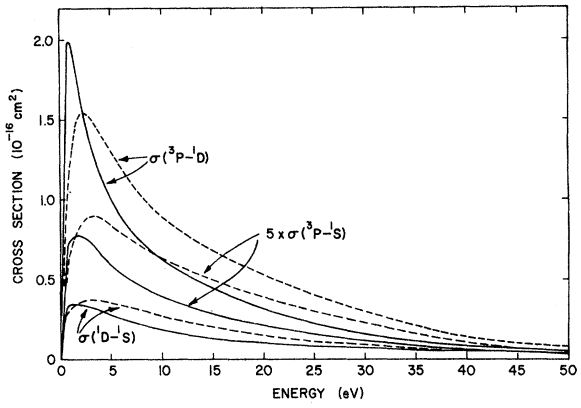

FIG. 1. Variation of inelastic cross sections with energy of incident electron above different thresholds for carbon. Threshold energies are 1.26, 2.68, and 1.42 eV for transitions ^3P–^1D, ^3P–^1S, and ^1D–^1S, respectively. Solid curves represent present calculations. Dashed curves represent results of Smith *et al.* (Ref. 2).

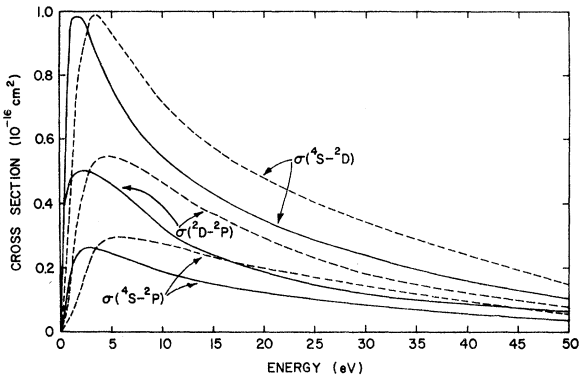

FIG. 2. Variation of inelastic cross sections with energy of incident electron above different thresholds for nitrogen. Threshold energies are 2.38, 3.57, and 1.19 eV for transitions ^4S–^2D, ^4S–^2P, and ^2D–^2P, respectively. Solid and dashed curves as in Fig. 1.

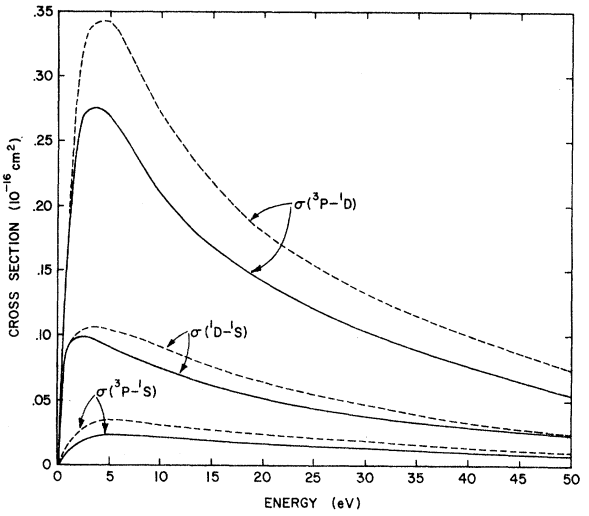

FIG. 3. Variation of inelastic cross sections with energy of incident electron above different thresholds for oxygen. Threshold energies are 1.96, 4.18, and 2.22 eV for transitions ^3P–^1D, ^3P–^1S, and ^1D–^1S, respectively. Solid and dashed curves as in Fig. 1.

TABLE II. Coefficients A for $E>40$ eV, for asymptotic behavior $\sigma(n,n')=Af(E)$, where energy in eV, cross section in units of 10^{-16} cm^2, and $f(E)$ has form: (a) $E^{-1}\ln E$; (b) E^{-1}; and (c) E^{-3}.

Atom	n	n'	A	$f(E)$
C	^3P	^1D	5950	(c)
	^3P	^1S	732	(c)
	^1D	^1S	2.14	(b)
N	^4S	^2D	12800	(c)
	^4S	^2P	4340	(c)
	^2D	^2P	1.20	(a)
O	^3P	^1D	7500	(c)
	^3P	^1S	900	(c)
	^1D	^1S	1.20	(b)

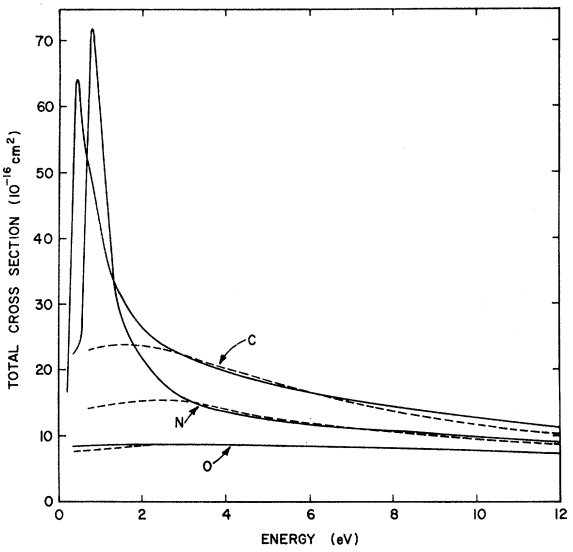

FIG. 4. Energy variation of total cross sections for electrons incident on carbon, nitrogen, and oxygen atoms. Solid and dashed curves as in Fig. 1.

agreement.[9] We find that below 1.6 eV the theoretical cross section is dominated by a resonance feature, which did not appear in our earlier calculation. A similar low-energy resonance is now obtained in the e^--C system. These features have an important influence on low-energy cross sections, and will be discussed in greater detail in the next section. Thus the main effect of the corrections to our treatment of Ψ_0 in Eq. (1) is the discovery of some low-energy shape resonances in the elastic scattering of carbon and nitrogen.

IV. SHAPE RESONANCES

In Fig. 4, the elastic cross sections for scattering of electrons by carbon and nitrogen are each dominated by a low-energy resonance. In each case, the feature is a shape resonance which is supported essentially by the angular momentum barrier term, which corresponds to $l=1$, in the effective potential. The low-energy p-wave phase shifts for e^--N(^3P) and e^--C($^2D^0$) are given in Fig. 5. These phase shifts may be analyzed to obtain the position and width of the resonance.

In the absence of long-range forces, the threshold dependence of the eigenphase δ_l may be given by the Blatt-Jackson formula

$$k^{2l+1}\cot\delta_l = -1/a + \tfrac{1}{2} r_0 k^2 . \tag{12}$$

A resonance, or a pole in the T matrix, occurs when $\cot\delta_l = i$, since

$$T = 2ie^{i\delta_l}\sin\delta_l = 2i/(\cot\delta_l - i) . \tag{13}$$

Thus $ik^{2l+1} = -1/a + \frac{1}{2} r_0 k^2$,

or $k^2 = k_r^2 - \frac{1}{2} i\Gamma$, (14)

where the resonance position and width are given by

$$k_r^2 = 2/ar_0 \tag{15}$$

and $\Gamma = -4k^{2l+1}/r_0$. (16)

From Eq. (13) we obtain

$$T = \frac{2ik^{2l+1}}{-1/a + \frac{1}{2} r_0 k^2 - ik^{2l+1}}$$

$$= \frac{i\Gamma}{(k_r^2 - k^2) - i\Gamma/2} . \tag{17}$$

The width in Eq. (16) is obviously energy-dependent, so we choose to define the width of the resonance at the resonance energy k_r^2. Thus

$$\Gamma = -(4/r_0)(2/ar_0)^{l+\frac{1}{2}} . \tag{18}$$

This definition is commonly used in the literature.

In our analysis of the phase shifts given in Fig. 5, we plot $k^3\cot\delta_1$ versus k^2 in order to obtain the scattering length a and the effective range r_0. Hence we obtain $k_r^2 = 0.065\,77$ Ry and $\Gamma = 0.046\,88$ Ry for e^--N(^3P), and $k_r^2 = 0.036\,10$ Ry and $\Gamma = 0.033\,45$ Ry for e^--C($^2D^0$). There is a slight deviation from a straight line in a plot of $k^3\cot\delta_1$ versus k^2 for the e^--C($^2D^0$) system, due to the presence of a small long-range quadrupole term, which is included in the theory. Thus the threshold dependence of the $l=1$ phase shift should be modified slightly. We have ignored this small effect, and feel that the use of the simple Blatt-Jackson formula should give a good indication of the position and width of the resonance.

There is no direct evidence that the ground state of the atomic-nitrogen negative ion is stable. Thus we believe that the resonance in the e^--N(^3P) sys-

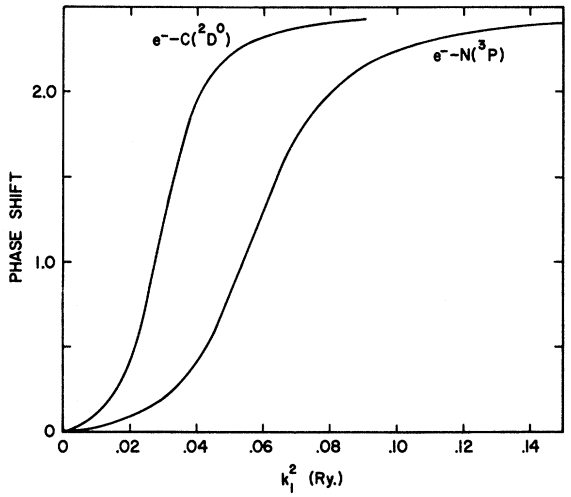

FIG. 5. Phase shift for the p wave versus energy (in Ry) for e^--C($^2D^0$) and e^--N(^3P) systems.

tem corresponds to the negative-ion state lying in the continuum. It is also most probably the state which is reached in the dissociation of the low-energy $^2\pi_g$ resonance state of N_2^-. Polarization terms are not included in our calculation. The inclusion of such terms would make the potential more attractive, and as a result the energy of the resonance would be lowered and its width narrowed. However, it is doubtful whether the polarizability would give enough attraction to cause the $N^-(^3P)$ state to become stable.

We have also calculated the position of the first and second excited states of N^-, relative to the ground state of atomic nitrogen. These ^1D and ^1S states lie at 0.16842 and 0.28811 Ry. Hence, we find that the ratio of the energy differences $(^1D\text{-}^1S)/(^3P\text{-}^1D)$ is 1.166. In the ^1D case, the lowest state of N with which a p electron can couple is the $^2D^0$ state, which is 0.17517 Ry above $N(^4S^0)$. However, in the ^1S case, the lowest state of atomic nitrogen which is allowed is the $^2P^0$ state. This lies 0.26276 Ry above $N(^4S^0)$, and so causes a low-energy shape resonance of width 0.02210 Ry in elastic scattering of electrons from $^2P^0$ state of atomic nitrogen.

We note that the $O^-(^2P^0)$ state is stable in our calculation, and so it does not produce a low-energy resonance effect. This accounts for the good agreement with Smith *et al.*[2] for elastic scattering of electrons from ground-state oxygen atoms.

Experimental results of Hall and Siegel[10] indicate that the first excited state of C^- is weakly bound, with a binding energy of ~0.05 eV. Our results show that the resonance in the $e^-\text{-}C(^2D^0)$ system corresponds to the excited negative ion lying in the continuum at ~0.5 eV above threshold. The atomic polarizability of carbon[11] is $14.5a_0^3$ compared with $7.6a_0^3$ for nitrogen,[12] thus the effect of polarization on carbon should be larger than on nitrogen, and may be sufficient to stabilize the $C^-(^2D^0)$ state.

V. ELECTRON-ION RESULTS

Our calculations on electron-ion scattering are carried out with the self-consistent-field (SCF) functions of Roothaan and Kelly.[13] We use the Hartree-Fock energy for the ground state of the ions and experimental values[14] for the energy differences between the terms. The ground-state configurations of the ions O^+, N^+, and O^{++} have three terms which we will denote, in order of increasing energy, by $n=1$, 2, and 3. The collision strengths $\Omega(n,n')$ are dimensionless parameters which are related to the collision cross sections $\sigma(n,n')$ through

$$\sigma(n,n') = (\pi/k_n^2\omega_n)\Omega(n,n'),$$

where ω_n is the statistical weight of the initial state, and k_n^2 is the energy of the incident electron in the nth channel.

In Table III we give our values for the collision strengths for $k_3^2=0$, together with the results of Saraph *et al.*[15] and Czyzak *et al.*[16] The dominant contributions to $\Omega(1,2)$ and $\Omega(1,3)$ for $2p^q$ ions come from p waves, and Saraph *et al.* and Czyzak *et al.* have used an improved form of the exact resonance approximation to calculate these contributions. For the other partial waves, they have used the distorted-wave approximation, whereas we have solved the close-coupling equations numerically for all partial waves.

The energy dependence of the collision strengths $\Omega(1,2)$, $\Omega(1,3)$, and $\Omega(2,3)$ respectively, is given in Figs. 6–8 for the ions O II, N II, and O III.

TABLE III. Collision strengths $\Omega(n,n')$ for $k_3^2=0$.

Ion	n	n'	This paper	Ref. 15	Ref. 16
N II	^3P	^1D	2.98	3.14	• • •
	^3P	^1S	0.395	0.342	• • •
	^1D	^1S	0.410	0.376	• • •
O III	^3P	^1D	2.53	2.39	• • •
	^3P	^1S	0.360	0.335	• • •
	^1D	^1S	0.325	0.310	• • •
O II	^4S	^2D	1.57	• • •	1.43
	^4S	^2P	0.475	• • •	0.428
	^2D	^2P	1.77	• • •	1.70

In our calculation of $\Omega(1,2)$ we have included only open channels in the expansion of the total wave function for the electron-ion system, so we do not obtain any resonance structure for electron energies less than the $n=3$ threshold. This structure

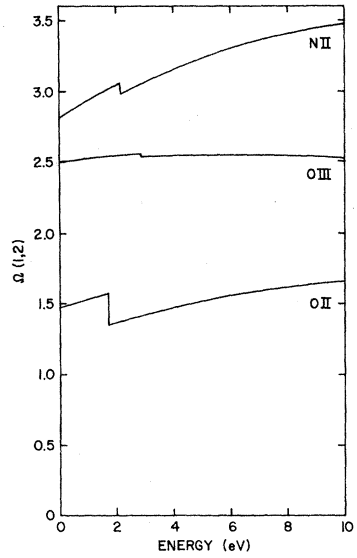

FIG. 6. Energy variation of collision strength $\Omega(1,2)$ for electrons incident on N^+, O^+, and O^{++} ions.

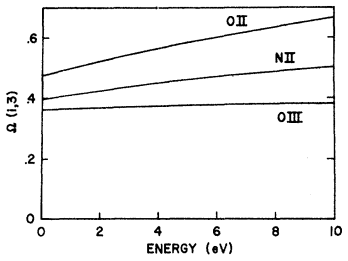

FIG. 7. Energy variation of collision strength $\Omega(1,3)$ for electrons incident on N^+, O^+, and O^{++} ions.

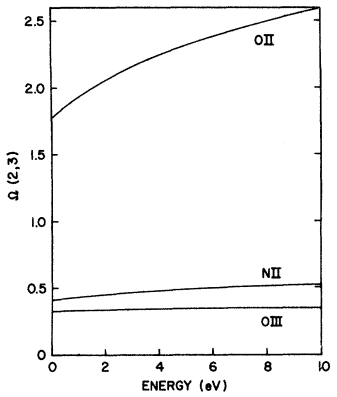

FIG. 8. Energy variation of collision strength $\Omega(2,3)$ for electrons incident on N^+, O^+, and O^{++} ions.

is found only when closed channels are included in the expansion. For example, when these channels were included by Henry[17] in a calculation of photon absorption by atomic oxygen, the resulting cross sections exhibited a resonance behavior. The omission of closed channels leads to a discontinuity in the collision strength at $k_3^2 = 0$. We note that as the $n = 3$ threshold is approached from lower energies, the value of $\Omega(1,2)$ is larger than that calculated when k_3^2 approaches zero from above. This is to be expected since some flux can escape through the additional open channels for energies above the $n = 3$ threshold.

VI. CONCLUSIONS

When the correct expressions for $V_i(r)$ and E_{N+1} are used, the peaks in electron-atom inelastic cross sections occur at lower energies than those calculated by Smith *et al.*,[2] and also the magnitude of the cross sections is lower at high energies.

Low-energy shape resonances are found in elastic scattering of electrons by ground-state carbon and nitrogen atoms. These resonances occur above threshold at ~0.5 eV for carbon and ~0.9 eV for nitrogen, with widths of approximately 0.45 and 0.64 eV, respectively. The experimental indications are that the inclusion of polarization terms may lead to the lowering of the resonance energy in the e^--$C(^2D^0)$ state, so that the state becomes stable. However, we feel that the polarization terms are unlikely to provide sufficient attraction to stabilize the ground state of the atomic-nitrogen negative ion. An interesting calculation would be to include polarization terms in addition to Ψ_0 terms in expansion (1).

The results of Saraph *et al.*[15] and Czyzak *et al.*[16] are found to be in good agreement with the present results for collision strengths for O II, N II, and O III ions, where comparison is possible.

ACKNOWLEDGMENTS

The authors are indebted to Professor M. J. Seaton for discussions which led to the discovery of the error in the original formulation. We also thank Drs. L. M. Branscomb and J. L. Hall for information concerning the electron affinity of the excited carbon negative ion.

---

†Work supported, in part, by the Physics Branch, U. S. Office of Naval Research, Washington, D. C., under Contract No. F6 1052-68-C-0012.

*Contribution No. 379 from the Kitt Peak National Observatory.

‡Operated by the Association of Universities for Research in Astronomy, Inc., under contract with the National Science Foundation.

[1]K. Smith, R. J. W. Henry, and P. G. Burke, Phys. Rev. 147, 21 (1966).

[2]K. Smith, R. J. W. Henry, and P. G. Burke, Phys. Rev. 157, 51 (1967).

[3]P. G. Burke and K. Smith, Rev. Mod. Phys. 34, 458 (1962).

[4]K. Smith, M. J. Conneely, and L. A. Morgan, Phys. Rev. 177, (1968).

[5]F. R. Innes, private communication; and J. Math. Phys. 8, 816 (1967).

[6]G. Sunshine, B. B. Aubrey, and B. Bederson, Phys. Rev. 154, 1 (1967).

[7]R. J. W. Henry, Phys. Rev. 162, 56 (1967).

[8]R. H. Neynaber, L. L. Marino, E. W. Rothe, and S. M. Trujillo, Phys. Rev. 129, 2069 (1963).

[9]R. J. W. Henry, Phys. Rev. 172, 99 (1968).

[10]J. Hall and M. Siegel, private communication.

[11]A. Dalgarno and D. Parkinson, Proc. Roy. Soc. (London) A250, 422 (1959).

[12]R. A. Alpher and D. R. White, Phys. Fluids 2, 153 (1959).

[13]C. C. J. Roothaan and P. S. Kelly, Phys. Rev. 131, 1177 (1963).

[14]C. E. Moore, Atomic Energy Levels, National Bureau of Standards Circular No. 467 (U. S. Government Printing Office, Washington, D. C., 1949), Vol. 1.

[15]H. E. Saraph, M. J. Seaton, and J. Shemming, Proc. Phys. Soc. (London) 89, 27 (1966).

[16]S. J. Czyzak, T. K. Krueger, H. E. Saraph, and J. Shemming, Proc. Phys. Soc. (London) 92, 1146 (1967).
[17]R. J. W. Henry, Planetary Space Sci. 16, (1968).

PHYSICAL REVIEW VOLUME 178, NUMBER 1 5 FEBRUARY 1969

Ionization of the Aluminum *K* Shell by Low-Energy Hydrogen and Helium Ions*

Werner Brandt and Roman Laubert
Department of Physics, New York University, New York, New York 10003
(Received 10 October 1968)

The yields for characteristic *K*-shell x rays in aluminum are measured as produced by H^1, He^3, and He^4 ions in the energy range 25–200 keV. The ionization cross sections deduced from these data are in detailed agreement with the theory, if the Coulomb deflection of the incoming particle by the target nucleus and the binding of the *K*-shell electrons to the incoming particle are included in the Born approximation.

INTRODUCTION

Until very recently, measurements of ionization cross sections of inner atomic shells by heavy charged particles were essentially limited to protons.[1] In a previous paper,[2] data on *K*-shell ionization cross sections of Mg, Al, and Cu were reported for low-energy hydrogen and helium atoms. It was shown that the large discrepancies between theory and experiment found earlier for protons[3] can be removed if, in addition to the effect of the Coulomb deflection of the incoming particle by the target nucleus, one incorporates the binding of the target electrons to the moving particle. The present paper reports new experimental data to test in detail on aluminum this expanded theory.

EXPERIMENTAL

The apparatus is similar to that described earlier.[2] An ion beam, after characterization by particle energy and mass, impinges on a thick target of high-purity aluminum. The target is inclined by 45° with respect to the ion beam axis and to the line of sight of a proportional counter. The target is heated to 150°C to suppress carbon deposition and insulated from the ground to measure the incident particle current accurately. The x rays emitted from the target are viewed by a flow-mode proportional counter whose output is connected to a multichannel analyzer. The total x ray yield is obtained from an appropriate integration over the spectrum as recorded for preset values of the integrated beam current.

RESULTS AND DISCUSSION

From the measurements of the Al (*K*) x ray yield Y, one extracts the x-ray production cross section $\sigma_x(E_1)$ in a standard manner by the formula[1]

$$\sigma_x(E_1)=\frac{1}{N_2}\left[\left(\frac{dY(E)}{dE}\right)_{E_1} S_2(E_1)+\mu_2 Y(E_1)\right], \quad (1)$$

and calculates the *K*-shell ionization cross section σ_K according to

$$\sigma_K(E_1)=\sigma_x(E_1)/\gamma_K. \quad (2)$$

E_1 is the energy of the incoming particles, N_2 the density of target atoms, $S_2(E_1)$ the stopping power of the target for particles of energy E_1, μ_2 the absorption coefficient of the target for its own characteristic x rays, and γ_K the *K*-shell fluoresence yield. The differentiation of the experimental yield curves with respect to energy introduces an uncertainty of ~15%, which is comparable with the uncertainty introduced by the stopping power. We used recent stopping-power data[4–6] and data obtained in this laboratory.[7] The ionization cross sections in absolute units are calculated by normalizing our data to the ionization cross section $\sigma_K=53$ b reported by Khan *et al.*[3] for protons at 100 keV. This cross section is obtained by assuming that $\gamma_K=0.03$, independent of the atomic number and the energy of the incoming particle. The uncertainty of this value is ±30%.[8]

The resulting *K*-shell ionization cross sections for H^1, He^3, and He^4 on aluminum are shown in Figs. 1–3, respectively. The large error bars represent the uncertainty in the absolute cross sections, the small error bars indicate the uncertainty of the points relative to each other. The data for protons on aluminum (cf. Fig. 1) agree with the results of Khan *et al.*[3] at all energies.